



## Comparison of finite difference and finite element solutions to the variably saturated flow equation

M.J. Simpson<sup>a</sup>, T.P. Clement<sup>a,b,\*</sup>

<sup>a</sup>Centre for Water Research, The University of Western Australia, Nedlands, WA 6907, Australia

<sup>b</sup>Department of Civil Engineering, Auburn University, AL 36849, USA

Received 30 November 2001; revised 5 July 2002; accepted 19 July 2002

### Abstract

Numerical solutions to the equation governing variably saturated flow are usually obtained using either the finite difference (FD) method or the finite element (FE) method. A detailed comparison of these methods shows that the main difference between them is in how the numerical schemes spatially average the variation of material properties. Further differences are also observed in the way that flux boundaries are represented in FE and FD methods. A modified finite element (MFE) algorithm is used to explore the significance of these differences. The MFE algorithm enables a direct comparison with a typical FD solution scheme, and explicitly demonstrates the differences between FE and FD methods. The MFE algorithm provides an improved approximation to the partial differential equation over the usual FD approach while being computationally simpler to implement than the standard FE solution. One of the main limitations of the MFE algorithm is that the algorithm was developed by imposing several restrictions upon the more general FE solution; however, the MFE is shown to be preferable over the usual FE and FD solutions for some of the test problems considered in this study. The comparison results show that the FE (or MFE) solution can avoid the erroneous results encountered in the FD solution for coarsely discretized problems. The improvement in the FE solution is attributed to the broader hydraulic conductivity averaging and differences in the representation of flux type boundaries.

© 2002 Published by Elsevier Science B.V.

*Keywords:* Variably saturated flow; Finite difference; Finite element; Numerical solution; Unsaturated flow; Groundwater

### 1. Introduction

Due to the non-linear physical processes associated with unsaturated conditions, the governing conservation equations for variably saturated flow problems are complex. Therefore, the solution of the governing equation is sought using numerical techniques, of which finite difference (FD) and finite element

(FE) methods are two popular schemes (Wang and Anderson, 1982; Zheng and Bennett, 1995). Variations of the standard FD and FE methods, such as the sub-domain FE method have also been successfully used to solve these problems (Cooley, 1983). The choice of using either an FD or FE method for the solution of variably saturated flow problems is largely personal and proponents of a particular method can easily support the strengths of their preferred solution strategy. This can cause problems when a choice has to be made between these approaches, as it is difficult to objectively compare the methods in a tangible manner.

\* Corresponding author. Address: Department of Civil Engineering, Auburn University, AL 36849, USA.

E-mail address: [clement@eng.auburn.edu](mailto:clement@eng.auburn.edu) (T.P. Clement).

This difficulty is further amplified because of the rich history of analysts who have consistently promoted one approach over the other. Hence, a study to compare the performance of these methods for several variably saturated flow problems is required so that a judgment of the preferred solution method can be identified using a sound physical basis.

Previous investigations directly comparing FE and FD formulations for the solution of variably saturated flow problems are limited. Philosophical discussions comparing the FE and FD methods in a general context are available, however these are constrained for making qualitative comparisons and provide little insight into the practical differences observed in the use of these techniques. For example, Gray (1984) presented a comprehensive analysis comparing FE and FD techniques in a general context, while Neumann et al. (1975) made some qualitative comments upon the differences in FE and FD approaches for the solution of variably saturated flow problems; however, no quantitative analysis was invoked.

The differences in the performance of FE and FD techniques for variably saturated flow in one-dimensional problems have been more thoroughly analyzed. For example Hayhoe (1978) compared FE and FD solutions to the one-dimensional, horizontal, water content form of the variably saturated flow equation. He concluded that a linear FE solution was preferable to a higher order FE solution, as well as noting that some improvement to the usual FD solution was obtained with alternative inter-nodal hydraulic conductivity averaging schemes. Van Genuchten (1982) compared an FD formulation and several FE formulations for the solution of one-dimensional variably saturated flow and solute transport. This work gave a comprehensive description for using several FE procedures to solve variably saturated, coupled flow and solute transport problems. More recently, Celia et al. (1990) compared one-dimensional FE and FD solutions to the variably saturated flow equation and showed that the results were dependent upon the method of temporal discretization chosen for the FE approach. These analyses are limited because of the focus upon one-dimensional problems. We aim to show that the true differences in FE and FD solutions are more pronounced in higher dimensional problems and therefore cannot be effectively deduced from these past one-dimensional studies.

The objective of this study is to compare the efficiency of FD and FE methodologies for solving the two-dimensional variably saturated flow equation. In particular, we compare the performance of two specific methods for the implementation of the FE and FD algorithms. This comparison motivated the development of a modified finite element (MFE) algorithm that enabled an explicit analysis of the significance of the differences between FE and FD solutions of two-dimensional variably saturated flow problems.

## 2. Background

### 2.1. Governing equation

The governing equation for variably saturated flow within a homogeneous, isotropic two-dimensional porous medium is (Clement et al., 1994):

$$\begin{aligned} \frac{\theta}{\phi} S_s \frac{\partial \psi}{\partial t} + \frac{\partial \theta}{\partial t} \\ = \frac{\partial}{\partial x} \left\{ K(\theta) \frac{\partial \psi}{\partial x} \right\} + \frac{\partial}{\partial z} \left\{ K(\theta) \frac{\partial \psi}{\partial z} \right\} + \frac{\partial K(\theta)}{\partial z} \end{aligned} \quad (1)$$

where  $S_s[L^{-1}]$  is the specific storage of the porous medium,  $\psi[L]$  is the pressure head,  $\theta$  is the water content,  $\phi$  is the porosity,  $K(\theta)[LT^{-1}]$  is the hydraulic conductivity,  $t[T]$  is time and  $x$  and  $z$  are the Cartesian coordinates.

Eq. (1) describes variably saturated flow under the conditions that (1) the air phase in the unsaturated zone does not interact with the fluid, and (2) the spatial distribution of fluid density is invariant.

### 2.2. Finite element algorithm

#### 2.2.1. Triangular elements

We used linear triangular elements to formulate the FE solution in this study. Alternatively shaped or higher order elements may also be used; however, linear triangular elements are known to produce a good solution to similar problems and are the simplest two-dimensional element that allows analytical analysis (Seegerlind, 1984; Cooley, 1992). The typical triangular element and nodal structure used in this study are shown in Fig. 1. A standard linear interpolation scheme

is used to form the trial solution as described by

$$\hat{\psi}(x, z) = \psi_r N_r + \psi_s N_s + \psi_t N_t \quad (2)$$

where,

$$N_r = \frac{1}{2A} [a_r + b_r x + c_r z],$$

$$N_s = \frac{1}{2A} [a_s + b_s x + c_s z],$$

$$N_t = \frac{1}{2A} [a_t + b_t x + c_t z], \quad a_r = x_s z_t - x_t z_s,$$

$$b_r = z_s - z_t, \quad c_r = x_t - x_s, \quad a_s = x_t z_r - x_r z_t,$$

$$b_s = z_t - z_r, \quad c_s = x_r - x_t, \quad a_t = x_r z_s - x_s z_r,$$

$$b_t = z_r - z_s, \quad c_t = x_s - x_r$$

where  $\hat{\psi}[L]$  is the interpolated pressure head,  $\psi_r, \psi_s$  and  $\psi_t[L]$  are the discrete values of the pressure head at the element vertices,  $N_r, N_s$  and  $N_t$  are the linear shape functions which depend upon the Cartesian coordinates  $(x, z)$  of the element vertices, and  $A[L^2]$  is the area of the element. Note that the terms  $a_r, a_s, a_t, b_r, b_s, b_t, c_r, c_s$  and  $c_t$  are traditionally used in triangular interpolation schemes to keep the notation succinct (Segerlind, 1984).

### 2.2.2. Galerkin finite element solution

The Galerkin solution technique assumes a trial solution to the partial differential equation. The residual error produced by the trial solution weighted by each shape function is then minimized at each computational node to form an algebraic analogue to the partial differential equation. The residual equation for element  $e$  takes the form:

$$\begin{aligned} \begin{Bmatrix} R_r^e \\ R_s^e \\ R_t^e \end{Bmatrix} &= \int_A \begin{Bmatrix} N_r^e \\ N_s^e \\ N_t^e \end{Bmatrix} \left[ \frac{\partial}{\partial x} \left\{ K(\theta) \frac{\partial \hat{\psi}}{\partial x} \right\} + \frac{\partial}{\partial z} \left\{ K(\theta) \frac{\partial \hat{\psi}}{\partial z} \right\} \right. \\ &\quad \left. + \frac{\partial K(\theta)}{\partial z} - \frac{\partial \hat{\theta}}{\partial t} - \frac{\hat{\theta}}{\phi} S_s \frac{\partial \hat{\psi}}{\partial t} \right] dA \end{aligned} \quad (3)$$

where  $A$  refers to the area of element  $e$ ,  $\{N^e\}$  are the shape functions associated with the element and  $\{R^e\}$  are the components of the nodal residuals associated with element  $e$ . Summing the residual components of a particular node arising from the surrounding patch of elements, and then forcing the residual to zero makes the trial solution approximate the actual solution in a discrete sense at a particular node.

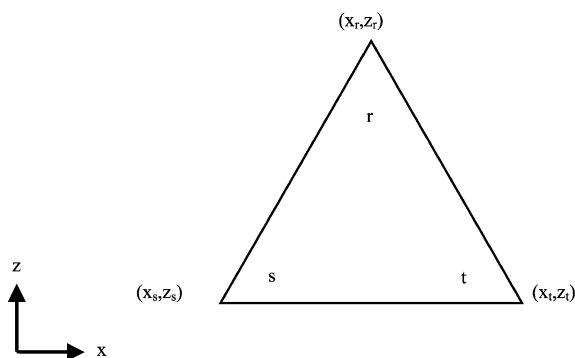


Fig. 1. Linear triangular element.

Eq. (3) is integrated using standard techniques to develop the element matrix equations (Eisenberg and Malvern, 1973; Segerlind, 1984). The non-linear equations are linearized by the introduction of a Picard iteration scheme (Cooley, 1983; Celia et al., 1990); and mass lumping is used to develop the capacitance matrix (Neumann, 1973; Celia et al., 1990). The resulting residual equation is:

$$\begin{aligned} \begin{Bmatrix} R_r^e \\ R_s^e \\ R_t^e \end{Bmatrix} &= - \frac{(K_r^m + K_s^m + K_t^m)}{12A} \begin{bmatrix} b_r^2 & b_r b_s & b_r b_t \\ b_s b_r & b_s^2 & b_s b_t \\ b_t b_r & b_t b_s & b_t^2 \end{bmatrix} \\ &\times \begin{Bmatrix} \psi_r^{m+1} \\ \psi_s^{m+1} \\ \psi_t^{m+1} \end{Bmatrix} - \frac{(K_r^m + K_s^m + K_t^m)}{12A} \\ &\times \begin{bmatrix} c_r^2 & c_r c_s & c_r c_t \\ c_s c_r & c_s^2 & c_s c_t \\ c_t c_r & c_t c_s & c_t^2 \end{bmatrix} \begin{Bmatrix} \psi_r^{m+1} \\ \psi_s^{m+1} \\ \psi_t^{m+1} \end{Bmatrix} \\ &+ \frac{(c_r K_r^m + c_s K_s^m + c_t K_t^m)}{6} \begin{bmatrix} 1 \\ 1 \\ 1 \end{bmatrix} \\ &- \frac{A}{3} \begin{bmatrix} 1 & 0 & 0 \\ 0 & 1 & 0 \\ 0 & 0 & 1 \end{bmatrix} \begin{Bmatrix} \theta_r^{m+1} \\ \theta_s^{m+1} \\ \theta_t^{m+1} \end{Bmatrix} - \frac{AS_s}{3\phi} \\ &\times \begin{bmatrix} \theta_r^m & 0 & 0 \\ 0 & \theta_s^m & 0 \\ 0 & 0 & \theta_t^m \end{bmatrix} \begin{Bmatrix} \psi_r^{m+1} \\ \psi_s^{m+1} \\ \psi_t^{m+1} \end{Bmatrix} + \begin{Bmatrix} \text{flux}_r \\ \text{flux}_s \\ \text{flux}_t \end{Bmatrix} \end{aligned} \quad (4)$$

Note that the above system forms the element level equations for the two-dimensional variably saturated flow equation. The dot above the entries represents a temporal derivative, while the superscript  $m$  refers to the previous Picard iteration level.

For the implementation of Eq. (4) in a standard FE code, the terms are evaluated in an element-by-element fashion and the resulting equations can be assembled together using the direct stiffness method to yield a set of linear equations (Segerlind, 1984). The linear system can be solved using a standard matrix solver (Istok, 1989).

### 2.3. Modified finite element algorithm

Typically, in the implementation of an FE code, all of the input data and manipulation are undertaken in terms of the element structure. Within the solution algorithm, the direct stiffness assembly procedure is used to transform the element information into a set of linear (or linearized) equations based upon the nodal structure. The equations are later solved to yield the discrete values of the dependent variable at the new iteration level.

Unfortunately, swapping between the element and nodal equation structure in this manner has two major limitations. Firstly, the process of preparation and assembly of the element information is cumbersome. Secondly, the internal computation required to achieve this element to nodal transformation is a lengthy computational process. Further, the element and node numbering systems are often ad hoc; hence the resulting linear equation system incorporates a large sparse matrix, which poses difficulties in terms of efficient storage and solution methods.

When an FE formulation is expanded upon an FD-like nodal arrangement, the two methods yield a similar discrete approximation to the partial differential equation (Zienkiewicz and Cheung, 1965; Pinder and Gray, 1976; Cooley, 1983). This observation is the motivation for the development of an MFE algorithm where the standard FE residual expression is developed in a nodal form instead of the usual element expression. The development of the FE solution using this modified strategy has two advantages. Firstly, the discrete MFE equations can be directly compared with a standard FD approximation

to explicitly elucidate the differences between the FD and FE methods. Secondly, the process of manually moving between the element formulation and the nodal expression is hoped to alleviate the problems associated with the computational assembly process in standard FE formulations, and lead to an efficient method to store and solve the resulting equations.

At this point the restrictions placed upon the MFE algorithm in its development should be noted. Since the MFE equations are to be expanded upon an FD grid, the MFE solutions shall be confined to discretizations with constant, but not necessarily equal nodal spacing in the  $x$  and  $z$  directions. Furthermore, since we are to directly compare the FD and MFE solutions, we restrict the MFE algorithm to situations where the material properties are not allowed to vary from element to element. These restrictions are necessary in order to enable a straightforward comparison between the MFE and FD solution techniques. It should be noted that these restrictions do impede the use of the MFE algorithm in comparison with the more general FE approach where both of these restrictions can be relaxed (Neumann, 1973; Cooley, 1983).

Once the FE equations have been expanded upon an FD grid, then a single governing relationship may be written for each node, and then applied throughout the grid. Developing the FE equations upon an FD-style grid is done by using two different triangular element orientations as shown in Fig. 2. These elements are used in conjunction with an FD grid as shown in Fig. 3. To compute the FE residual for the central node upon this grid, Eq. (4) must be written for each of the six elements that surround the central computational node. Since the components of the element matrices depend upon the orientation of the element, Eq. (4) must be reformulated to correspond to the two different element orientations. For elements 1, 3 and 5 which are all oriented in the same way, evaluating the element matrices in terms of the FD grid spacing yields a residual equation,

$$\begin{Bmatrix} R_r^e \\ R_s^e \\ R_t^e \end{Bmatrix} = -\frac{\Delta z^2 (K_r^m + K_s^m + K_t^m)}{12A} \begin{bmatrix} 0 & 0 & 0 \\ 0 & 1 & -1 \\ 0 & -1 & 1 \end{bmatrix} \begin{Bmatrix} \psi_r^{m+1} \\ \psi_s^{m+1} \\ \psi_t^{m+1} \end{Bmatrix}$$

$$\begin{aligned}
 & -\frac{\Delta x^2(K_r^m + K_s^m + K_t^m)}{12A} \begin{bmatrix} 1 & -1 & 0 \\ -1 & 1 & 0 \\ 0 & 0 & 0 \end{bmatrix} \begin{Bmatrix} \psi_r^{m+1} \\ \psi_s^{m+1} \\ \psi_t^{m+1} \end{Bmatrix} \\
 & + \frac{\Delta x(K_r^m - K_s^m)}{6} \begin{bmatrix} 1 \\ 1 \\ 1 \end{bmatrix} - \frac{A}{3} \begin{bmatrix} 1 & 0 & 0 \\ 0 & 1 & 0 \\ 0 & 0 & 1 \end{bmatrix} \begin{Bmatrix} \theta_r^{m+1} \\ \theta_s^{m+1} \\ \theta_t^{m+1} \end{Bmatrix} \\
 & - \frac{AS_s}{3\phi} \begin{bmatrix} \theta_r^m & 0 & 0 \\ 0 & \theta_s^m & 0 \\ 0 & 0 & \theta_t^m \end{bmatrix} \begin{Bmatrix} \psi_r^{m+1} \\ \psi_s^{m+1} \\ \psi_t^{m+1} \end{Bmatrix} + \begin{Bmatrix} \text{flux}_r \\ \text{flux}_s \\ \text{flux}_t \end{Bmatrix}. \quad (5)
 \end{aligned}$$

A similar expression can be obtained by evaluating Eq. (4) for elements 2, 4 and 6

$$\begin{aligned}
 \begin{Bmatrix} R_r^e \\ R_s^e \\ R_t^e \end{Bmatrix} &= -\frac{\Delta z^2(K_r^m + K_s^m + K_t^m)}{12A} \begin{bmatrix} 0 & 0 & 0 \\ 0 & 1 & -1 \\ 0 & -1 & 1 \end{bmatrix} \begin{Bmatrix} \psi_r^{m+1} \\ \psi_s^{m+1} \\ \psi_t^{m+1} \end{Bmatrix} \\
 & -\frac{\Delta x^2(K_r^m + K_s^m + K_t^m)}{12A} \begin{bmatrix} 1 & -1 & 0 \\ -1 & 1 & 0 \\ 0 & 0 & 0 \end{bmatrix} \begin{Bmatrix} \psi_r^{m+1} \\ \psi_s^{m+1} \\ \psi_t^{m+1} \end{Bmatrix} \\
 & + \frac{\Delta x(K_s^m - K_r^m)}{6} \begin{bmatrix} 1 \\ 1 \\ 1 \end{bmatrix} - \frac{A}{3} \begin{bmatrix} 1 & 0 & 0 \\ 0 & 1 & 0 \\ 0 & 0 & 1 \end{bmatrix} \begin{Bmatrix} \theta_r^{m+1} \\ \theta_s^{m+1} \\ \theta_t^{m+1} \end{Bmatrix} \\
 & - \frac{AS_s}{3\phi} \begin{bmatrix} \theta_r^m & 0 & 0 \\ 0 & \theta_s^m & 0 \\ 0 & 0 & \theta_t^m \end{bmatrix} \begin{Bmatrix} \psi_r^{m+1} \\ \psi_s^{m+1} \\ \psi_t^{m+1} \end{Bmatrix} + \begin{Bmatrix} \text{flux}_r \\ \text{flux}_s \\ \text{flux}_t \end{Bmatrix}. \quad (6)
 \end{aligned}$$

The expressions (5) and (6) are written by recognizing that the interpolation terms  $b_r, b_s, b_t, c_r, c_s$  and  $c_t$  can be

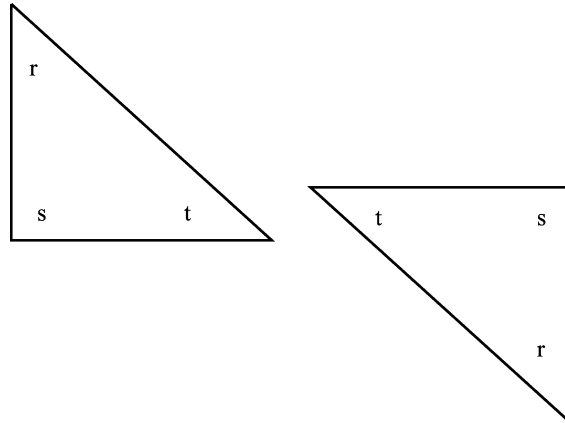


Fig. 2. Element orientation and node structure.

evaluated using the nodal spacings  $\Delta x$  and  $\Delta z$ . Although the terms in Eqs. (5) and (6) are almost identical, they really should not be compared with each other. This is because the two expressions are written upon completely different, unrelated elements. The choice of the element and node numbering is arbitrary. If an alternative element and node numbering were chosen, then intermediate expressions (5) and (6) would differ, but the final result would be identical. The current element and node numbering was chosen because it yielded the most compact intermediate equations.

Now that the FE relations for the specified element layout are established, they must be transferred to an FD grid, therefore the indices used in Eqs. (5) and (6) must be replaced by the corresponding FD nodal indices. The structure and nomenclature used for the FD-style expression are shown in Fig. 3. (Note that in the figure the FE notation is given in the interior of the elements and the FD notation is given on the exterior of the elements.) Since each element contributes one component of the residual at the central node, the total residual at the central node will be

$$R_{i,j} = R_s^1 + R_t^2 + R_r^3 + R_s^4 + R_t^5 + R_r^6 \quad (7)$$

where  $R_s^1$  is the residual component from the first element at the  $s$ th vertex,  $R_t^2$  is the residual component from the second element at the  $t$ th vertex and so on. Each of the residual components in Eq. (7) can be deduced from Eqs. (5) and (6). For example, for element 1, the  $s$ th vertex of the element will contribute a residual to the central computational

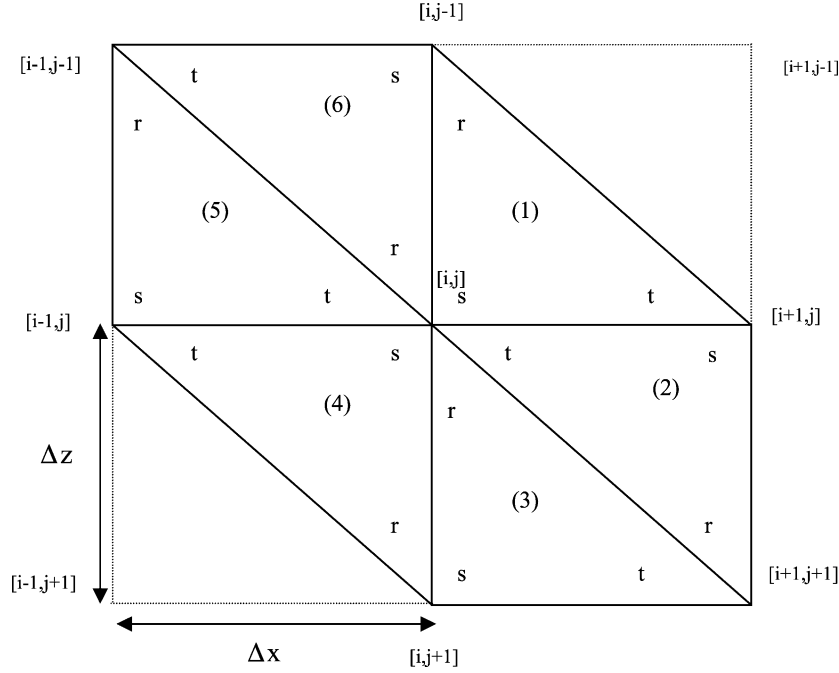


Fig. 3. Element topology used to define the MFE five-star computational molecule relationship.

node. Hence, the component of the residual expression comes from the  $R_s$  row of the FE relation (5) and using this information the residual  $R_s^1$  can be evaluated as

$$R_s^1 = \frac{-\Delta z^2}{12A} (K_s^m + K_t^m + K_r^m) (\psi_s^{m+1} - \psi_t^{m+1}) - \frac{A\theta_s^{m+1}}{3} - \frac{S_s A \theta_s^m \psi_s^{m+1}}{3\phi} + \frac{\Delta x}{6} (K_r^m - K_s^m) - \frac{\Delta x^2}{12A} (K_s^m + K_t^m + K_r^m) (\psi_s^{m+1} - \psi_r^{m+1}) \quad (8)$$

Now that the residual component of element 1 has been established we will move from the FE ( $r, s, t$ ) notation to the general FD ( $i, j$ ) notation to be consistent with FD terminology. This is accomplished by simply comparing the nodal indices in Fig. 3. Eq. (8) can be written in terms of the FD indices as:

$$R_{i,j}^1 = \frac{-\Delta z^2}{12A} (K_{i,j}^m + K_{i+1,j}^m + K_{i,j-1}^m) (\psi_{i,j}^{m+1} - \psi_{i+1,j}^{m+1}) - \frac{A\theta_{i,j}^{m+1}}{3} - \frac{S_s A \theta_{i,j}^m \psi_{i,j}^{m+1}}{3\phi} + \frac{\Delta x}{6} (K_{i,j-1}^m - K_{i,j}^m) - \frac{\Delta x^2}{12A} (K_{i,j}^m + K_{i+1,j}^m + K_{i,j-1}^m) (\psi_{i,j}^{m+1} - \psi_{i,j-1}^{m+1}) \quad (9)$$

Repeating this process of recognizing which vertex of elements 2–6 would contribute to the central node, and then expanding the corresponding relationship yields the remaining residual components for each element. Once each of the components of the element residual has been obtained, they can be substituted into Eq. (7) to develop a discrete form of the governing equation. This relationship is written in an FD-style format as

$$a\psi_{i,j-1}^{m+1} + b\psi_{i-1,j}^{m+1} + c\psi_{i,j}^{m+1} + d\psi_{i+1,j}^{m+1} + e\psi_{i,j+1}^{m+1} = f \quad (10)$$

where

$$a = \frac{\Delta x^2}{12A} (2K_{i,j}^m + 2K_{i,j-1}^m + K_{i+1,j}^m + K_{i-1,j-1}^m),$$

$$b = \frac{\Delta z^2}{12A} (2K_{i,j}^m + 2K_{i-1,j}^m + K_{i,j+1}^m + K_{i-1,j-1}^m),$$

$$d = \frac{\Delta z^2}{12A} (2K_{i,j}^m + 2K_{i+1,j}^m + K_{i,j-1}^m + K_{i+1,j+1}^m),$$

$$e = \frac{\Delta x^2}{12A} (2K_{i,j}^m + 2K_{i,j+1}^m + K_{i-1,j}^m + K_{i+1,j+1}^m),$$

$$c = -a - b - d - e,$$

$$f = 2A\theta_{i,j}^{m+1} + \frac{2A\theta_{i,j}^m S_s \psi_{i,j}^{m+1}}{\phi} - \frac{\Delta x}{6}(2K_{i,j-1}^m - 2K_{i,j+1}^m + K_{i+1,j}^m - K_{i+1,j+1}^m + K_{i-1,j-1}^m - K_{i-1,j}^m).$$

Eq. (10) is an FE approximation written at a general node within the domain.

Before applying Eq. (10) to solve a problem, the temporal derivative components must be expressed in terms of the dependent variable. This is achieved using a backward Euler stepping for the pressure storage term along with the modified Picard linearization procedure for the water content term (Celia et al., 1990). Note that the modified Picard linearization procedure is a specialization of the general linearization technique described by Cooley (1983). To make the equation compatible with the FD expression, the area of the element  $A[L^2]$  is expressed in terms of nodal spacing and then each term is divided through by  $(\Delta x \Delta z)$ . The resulting expression is

$$a\psi_{i,j-1}^{m+1,n+1} + b\psi_{i-1,j}^{m+1,n+1} + c\psi_{i,j}^{m+1,n+1} + d\psi_{i+1,j}^{m+1,n+1} + e\psi_{i,j+1}^{m+1,n+1} = f \quad (11)$$

where

$$a = \frac{1}{6\Delta z^2}(2K_{i,j}^{m,n+1} + 2K_{i,j-1}^{m,n+1} + K_{i+1,j}^{m,n+1} + K_{i-1,j-1}^{m,n+1}),$$

$$b = \frac{1}{6\Delta x^2}(2K_{i,j}^{m,n+1} + 2K_{i-1,j}^{m,n+1} + K_{i,j+1}^{m,n+1} + K_{i-1,j-1}^{m,n+1}),$$

$$d = \frac{1}{6\Delta x^2}(2K_{i,j}^{m,n+1} + 2K_{i+1,j}^{m,n+1} + K_{i,j-1}^{m,n+1} + K_{i+1,j+1}^{m,n+1}),$$

$$e = \frac{1}{6\Delta z^2}(2K_{i,j}^{m,n+1} + 2K_{i,j+1}^{m,n+1} + K_{i-1,j}^{m,n+1} + K_{i+1,j+1}^{m,n+1}),$$

$$c = -a - b - d - e - \frac{C_{i,j}^{m,n+1}}{\Delta t} - \frac{\theta_{i,j}^{m,n+1} S_s}{\Delta t \phi},$$

$$f = \frac{(\theta_{i,j}^{m,n+1} - \theta_{i,j}^n)}{\Delta t} - \frac{C_{i,j}^{m,n+1} \psi_{i,j}^{m,n+1}}{\Delta t} - \frac{\theta_{i,j}^{m,n+1} S_s \psi_{i,j}^n}{\Delta t \phi}$$

$$- \frac{1}{6\Delta z}(2K_{i,j-1}^{m,n+1} - 2K_{i,j+1}^{m,n+1} + K_{i+1,j}^{m,n+1} - K_{i+1,j+1}^{m,n+1}$$

$$+ K_{i-1,j-1}^{m,n+1} - K_{i-1,j}^{m,n+1})$$

where  $C[L^{-1}]$  is the capacity function, which is obtained by computing the slope of the water retention

curve. Note that the superscript  $n$  refers to the previous level of time integration, while the superscript  $n + 1$  refers to the values at the current (unknown) time increment.

Eq. (11) is the final form of the discrete MFE equation to be applied at an internal node. The structure of Eq. (11) defines a five-star computational molecule relationship that avoids the need for global nodal numbering as it relies only upon a local numbering scheme. Note the MFE approximation (11) can be compactly assembled into a pentadiagonal matrix equation that avoids the storage of zero entries; this approach is commonly employed in FD algorithms (Clement et al., 1994). This form of the MFE equations is useful as it allows a direct comparison to be made between two specific FE and FD methods so that an understanding of the working differences between these methods can be explicitly developed.

#### 2.4. Boundary conditions

Both Dirichlet and Neumann boundaries are considered. Dirichlet nodes occur where the pressure head is known a priori at some point on the domain boundary. Neumann boundaries occur where a value of the normal flux,  $q[LT^{-1}]$  is known at some location along the boundary. The methods for the implementation of Dirichlet and Neumann boundary condition are well known and have been documented for the general FE procedure (Segerlind, 1984). The use of these principles in the MFE discretization is a straightforward extension of the development of the interior node expression.

The implementation of Dirichlet boundaries in both FD and FE algorithms are identical. The implementation of Neumann boundaries however, is different. A Neumann boundary is incorporated into an FD algorithm by writing a discrete form of Darcy's law at the boundary node where the flux is known (Clement et al., 1994). In an FE algorithm, specified fluxes are incorporated into the flux vector (Eq. (4)) that results from the application of integration by parts upon the original element-level residual expression (Eq. (3)). These two approaches lead to different expressions at Neumann boundary nodes for FE and FD techniques. The mathematical details of these differences are discussed in Simpson (2002).

### 2.5. Theoretical comparison of finite difference and finite element solution algorithms

A standard, fully implicit in time and centered in space FD approximation for Eq. (1) can be written as (Clement et al., 1994)

$$a\psi_{i,j-1}^{m+1,n+1} + b\psi_{i-1,j}^{m+1,n+1} + c\psi_{i,j}^{m+1,n+1} + d\psi_{i+1,j}^{m+1,n+1} + e\psi_{i,j+1}^{m+1,n+1} = f \quad (12)$$

where

$$a = \frac{1}{2\Delta z^2} (K_{ij}^{m,n+1} + K_{i,j-1}^{m,n+1}),$$

$$b = \frac{1}{2\Delta x^2} (K_{ij}^{m,n+1} + K_{i-1,j}^{m,n+1}),$$

$$d = \frac{1}{2\Delta x^2} (K_{ij}^{m,n+1} + K_{i+1,j}^{m,n+1}),$$

$$e = \frac{1}{2\Delta z^2} (K_{ij}^{m,n+1} + K_{i,j+1}^{m,n+1}),$$

$$c = -a - b - d - e - \frac{C_{ij}^{m,n+1}}{\Delta t} - \frac{S_s}{\Delta t\phi},$$

$$f = \frac{(\theta_{ij}^{m,n+1} - \theta_{ij}^m)}{\Delta t} - \frac{C_{ij}^{m,n+1}\psi_{ij}^{m,n+1}}{\Delta t} - \frac{S_s\psi_{ij}^m}{\Delta t\phi} - \frac{1}{2\Delta z} (K_{i,j-1}^{m,n+1} - K_{i,j+1}^{m,n+1}).$$

In this study, the linear systems generated by both the FD and the MFE algorithms were solved using a bi-conjugate gradient method (Press et al., 1992). The multiplying routine was developed to take advantage of the penta-diagonal structure of the equations in both solutions.

A comparison of the discrete formulations (11) and (12) elucidates several important differences between the FE and FD approaches. In the discretization of the diffusive terms for the MFE algorithm, one of the shape function parameters in the MFE equation was always zero for each element. For example, in elements 1, 3 and 5, the  $b_r$  term from Eq. (2) was always zero as the  $s$  and  $t$  vertices in these elements have the same elevation ( $z$  value). This leads to several entries in the diffusive matrices being zero. The result of these zero entries has the convenient effect of making the residual at the central node

independent of the pressure head at the diagonal nodes. For example, in element 3 (Fig. 3), the southeast diagonal node is denoted as the  $r$ th node while the central node corresponds to the  $r$ th node. To obtain the residual expression for element 3 requires the expansion of the  $r$ th row of Eq. (5), which has two matrices involving the unknown pressure heads: one for the  $x$  diffusive term and the other for the  $z$  diffusive term. Since the (1,3) entry in the  $x$  diffusive matrix and the (3,3) entry in the  $z$  diffusive matrix are zeros, the residual expression at the central node becomes uncoupled from the pressure head at the diagonal node. This uncoupling is also observed for all other elements that are connected to the diagonal nodes. This implies that the residual at the central node is not explicitly dependent upon the current value of the dependent variable (the pressure head) on the northwest and southeast diagonal nodes. Therefore, the dependent variable is only accessed through the vertical and horizontal nodes, which are the same nodes used by a standard FD approach. The nodal value of the hydraulic conductivity however, is accessed at all nodes including the diagonal nodes. Therefore, the FE discretization naturally incorporates the influence of the hydraulic conductivity variation over a greater spatial area than does the FD approximation. This broader representation of the hydraulic conductivity differs from the standard FD approximation that only accesses the vertical and horizontal nodes. These kinds of observations have been previously noted (Cooley, 1983); however, the significance of these differences between the FE and FD solutions of the two-dimensional variably saturated flow equation has not been thoroughly analyzed.

It should be noted that the FD approximation used in this comparison study utilizes a specific kind of approximation to the partial differential equation. The work of Clement et al. (1994) resulted in a scheme where an arithmetic mean of the hydraulic conductivity was employed. Several researchers have found that alternative averaging schemes can improve the performance of FD approximations (Hayhoe, 1978; Haverkamp and Vauclin, 1981). However, we focused upon arithmetic averaging only as it is the most intuitive approach and it also allowed us to compare our results against standard published results from Clement et al. (1994).



The comparison of the discrete relationships (11) and (12) has several different implications. Firstly, since the nodal relationship for the MFE formulation is similar to the FD approximation in terms of how the dependant variable is accessed, it is possible to transform any working FD model into an equivalent MFE model with minimal effort. This transformation has the advantage that the MFE model can now take advantage of the penta-diagonal matrix storage posed by the form of Eq. (11). This avoids the use of sparse matrix storage methods and solution schemes. Secondly, the discrete formulations explicitly show how FE approximations naturally result in an intrinsic averaging scheme for the hydraulic conductivity over a broader spatial extent than the FD scheme.

### 3. Validation of modified finite element algorithm

In order to assess the computational differences between the MFE and FD algorithms, first the models must be validated. This was achieved by independently testing the MFE and FD algorithms against several benchmark problems. The benchmark results for the FD algorithm have been previously discussed in Clement et al. (1994). The results for the MFE algorithm are discussed here.

#### 3.1. Transient infiltration into a dry soil

The first test problem relates to a field example of variably saturated infiltration and solute transport. Van Genuchten (1982) provided a numerical solution to this field study which was completed by Warrick et al. (1971). Although this problem is a one-dimensional infiltration process, the solution was found upon a two-dimensional mesh. This was achieved by using a two-dimensional mesh with no-flow boundaries imposed upon the vertical sides of the mesh to reproduce the one-dimensional conditions. This allows for a one-dimensional problem to be solved while still exploring the impact of two-dimensional discretization effects. The use of one-dimensional problems to verify higher dimensional algorithms is a common validation strategy; for example, Segol (1976) used a one-dimensional problem to verify a three-dimensional coupled flow and solute transport model.

The water retention curve for the soil is given by:

$$\begin{aligned}\theta &= 0.6829 - 0.09524 \log_e |\psi|, & -29.484 \text{ cm} \leq \psi; \\ \theta &= 0.4531 - 0.02732 \log_e |\psi|, & 0.0 \leq \psi \leq -29.484 \text{ cm.}\end{aligned}\quad (13)$$

Similarly the hydraulic conductivity function was defined using the relations:

$$\begin{aligned}K &= 80,482.5 |\psi|^{-3.4095}, & -29.484 \text{ cm} \leq \psi; \\ K &= 21.5334 |\psi|^{-0.97814}, & 0.0 \leq \psi \leq -29.484 \text{ cm.}\end{aligned}\quad (14)$$

The initial conditions for the simulation are  $\theta(x, z, 0) = 0.2$  for  $60 \leq z \leq 125$  cm, and  $\theta(x, z, 0) = 0.15 + (z/1200)$ , for  $0 \leq z \leq 60$  cm (Van Genuchten, 1982). The flow was initiated using a Dirichlet boundary at the surface with  $\psi = -14.5$  cm; the base of the column was impervious to flow. Numerical simulations were performed with  $\Delta t = 0.01$  h, and use spatial discretizations of  $\Delta z = 2.5$  cm and  $\Delta x = 2.5$  cm. The wetting front profiles generated by the modified algorithm are superimposed upon the Van Genuchten (1982) solution in Fig. 4. The MFE algorithm captured both the position and shape of the wetting front after 2 and 9 h of infiltration.

#### 3.2. Transient water-table mounding problem

This example was used to verify a two-dimensional recharge problem involving spatially variable flux boundaries. The problem was based upon laboratory results presented by Vauclin et al. (1979), which reported the transient position of the phreatic surface in a laboratory scale soil box. The domain is a rectangular block 600 cm  $\times$  200 cm; the water table is initially located at a height of 65 cm from the base and the recharge occurs over a strip of the aquifer of 100 cm wide. A recharge of 355 cm/day was applied at the soil surface. Since the problem was symmetric, only the right hand side of the domain was modeled with a no flow boundary imposed along the axis of symmetry. No flow boundaries were also imposed along the lower and upper boundaries with the exception of the recharge zone. The right hand boundary is also modeled with a no flow boundary above the water table, and the nodes below the water

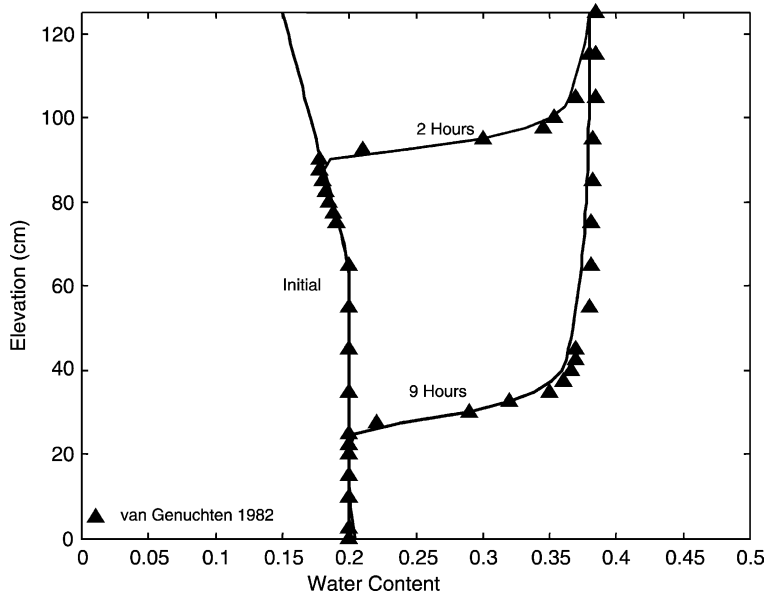


Fig. 4. Vertical movement of the transient wetting front as simulated with the MFE algorithm.

table are held at a hydrostatic pressure distribution. The water retention characteristics are simulated using the [Van Genuchten \(1980\)](#) model

$$\Theta = \left\{ \frac{m_v}{1 + (\alpha_v |\psi|)^{n_v}} \right\} \quad (15)$$

where  $\alpha_v [L^{-1}]$ ,  $n_v$  and  $m_v$  are the Van Genuchten parameters. The effective saturation  $\Theta$ , is then related to the moisture content of the soil by

$$\Theta = \frac{\theta - \theta_r}{\theta_s - \theta_r} \quad (16)$$

where  $\Theta$  is the effective saturation,  $\theta$  is the moisture content,  $\theta_r$  is the residual water content and  $\theta_s$  is the saturated water content or porosity of the porous media.

[Mualem's \(1976\)](#) model relating the unsaturated hydraulic conductivity to the effective saturation is used for the description of the hydraulic conductivity

$$K(\Theta) = K_s [1 - \{1 - \Theta^{(1/m_v)}\}^{m_v}]^2 \sqrt{\Theta} \quad (17)$$

where  $K(\Theta) [LT^{-1}]$  is the hydraulic conductivity,  $K_s [LT^{-1}]$  is the saturated hydraulic conductivity,  $\Theta$  is the effective saturation, and  $m_v$  is the Van Genuchten parameter. The modified algorithm was used with a regular grid discretized with  $\Delta x = 10.0$  cm and

$\Delta z = 5.0$  cm, the temporal discretization was  $\Delta t = 0.002$  h. An equivalent Van Genuchten model for the porous medium was described using  $\alpha_v = 3.3 \text{ m}^{-1}$  and  $n_v = 4.1$  which were identified by [Clement et al. \(1994\)](#). The value of the saturated hydraulic conductivity was  $K_{\text{sat}} = 840$  cm/day.

[Fig. 5](#) shows the spatial and temporal distribution of the phreatic surface predicted by the algorithm along with the data points from the experimental work. The profiles show that the algorithm is able to reproduce the transient water table positions quite accurately.

#### 4. Comparison of modified finite element and finite difference algorithms

Since the MFE and FD formulations have differences in the way which they approximate the partial differential equation, it is of interest to see if these differences can be observed in the numerical solution of a problem. For this comparison, the proposed MFE algorithm and the FD algorithm of [Clement et al. \(1994\)](#) were used to simulate two benchmark problems under varying spatial and temporal discretizations. The accuracy of the solutions in response

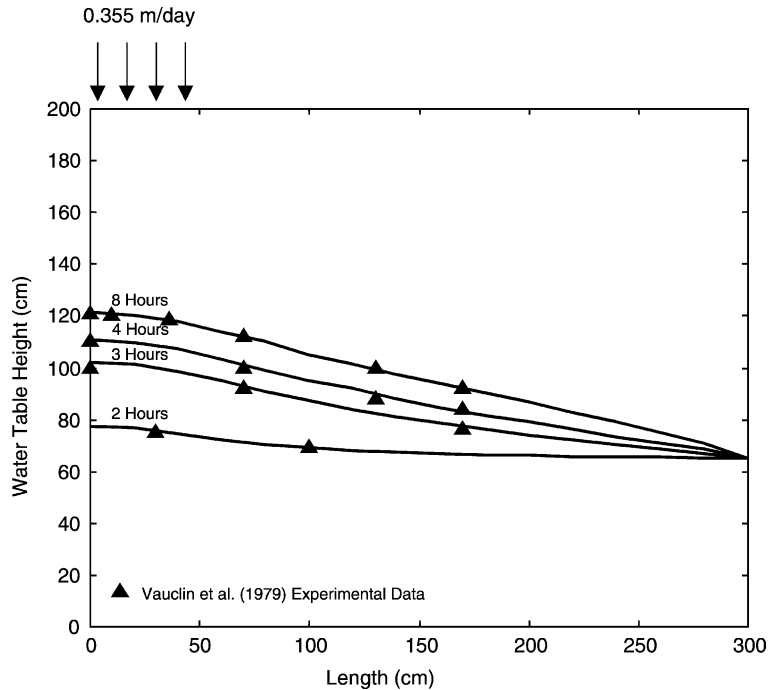


Fig. 5. Transient water table for the Vauclin infiltration problem as simulated by the MFE algorithm.

to the varying discretizations was directly measured through a comparison of the distribution of the pressure heads for each discretization against a fine solution. The ‘fine solution’ used for this purpose was the previously verified solution for each of the test problems generated using fine temporal and spatial discretizations. Note that the fine mesh solutions from the FD and MFE algorithms were indistinguishable. The deviation between the fine and several sets of coarse solutions are quantified using a root mean square error, defined as

$$\text{RMSE} = \sqrt{\frac{\sum_{i=1}^N (\psi_{\text{fine}} - \psi_{\text{coarse}})^2}{N}} \quad (18)$$

where RMSE is the root mean square error,  $\psi_{\text{coarse}}[\text{L}]$  is a test solution generated using a coarser grid,  $\psi_{\text{fine}}[\text{L}]$  is the true solution, and  $N$  is the total number of grid points.

In addition, a traditional mass balance approach was also used to track the numerical error. However, in several instances, the algorithms were able to maintain a good closure of mass in the domain even though the internal structure of the solution was

different from the fine solution. Therefore, in this work, we used the RMSE to quantify the deviations between coarse and fine solutions.

#### 4.1. Comparison of results for the field infiltration problem

The field infiltration problem was resolved using both the MFE and FD algorithms subject to spatial discretizations of  $\Delta z = 2.5, 5.0$  and  $12.5$  cm in conjunction with temporal discretizations of  $\Delta t = 0.01, 0.1$  and  $0.5$  h. The two-dimensional meshes were constructed using square grids with  $\Delta x = \Delta z$ .

Table 1 shows the comparison of the numerical error for different sets of discretizations. The error analysis shows the following trends: (1) the error from the MFE algorithm is consistently equivalent to that associated with the FD algorithm, and (2) the error increases for both MFE and FD methods as the mesh becomes increasingly coarse. Also, in general, the error decreases with a decrease in  $\Delta t$ ; however, it is difficult to generalize this trend because certain coarse meshes yielded reduced error with an increase in  $\Delta t$ .

Table 1  
Comparison of the MFE and FD solutions for the field infiltration problem

Run	$\Delta z$ (cm)	$\Delta t$ (h)	Time (h)	MFE error	FD error
1	2.5	0.01	2.0	0.000	0.001
2	2.5	0.10	2.0	0.002	0.002
3	2.5	0.50	2.0	0.009	0.009
4	5.0	0.01	2.0	0.008	0.008
5	5.0	0.10	2.0	0.006	0.006
6	5.0	0.50	2.0	0.012	0.012
7	12.5	0.01	2.0	0.023	0.023
8	12.5	0.10	2.0	0.021	0.021
9	12.5	0.50	2.0	0.017	0.017
10	2.5	0.01	9.0	0.000	0.000
11	2.5	0.10	9.0	0.001	0.001
12	2.5	0.50	9.0	0.008	0.008
13	5.0	0.01	9.0	0.006	0.006
14	5.0	0.10	9.0	0.005	0.005
15	5.0	0.50	9.0	0.008	0.008
16	12.5	0.01	9.0	0.022	0.023
17	12.5	0.10	9.0	0.021	0.021
18	12.5	0.50	9.0	0.018	0.018

Fig. 6 shows plots of the profiles generated with a coarse discretization along with the solution generated upon a fine mesh. Even at this relatively coarse discretization, there appears to be no advantage in using either the FD or MFE algorithms. Both the FD

and MFE solutions are identical; both profiles show errors as the shape of the wetting front is significantly smoothed in comparison to the fine mesh solution. This result agrees with Celia et al. (1990) who showed that mass-lumped, linear Galerkin FE approximations to one-dimensional problems are equivalent to the standard centered in space, fully implicit in time FD approximation. Further discussions of the effects of different boundary conditions for one-dimensional problems are discussed in Simpson (2002).

#### 4.2. Comparison of results for the transient water-table mounding problem

The original Vauclin example was modified slightly in order to allow the use of several uniform discretizations. The domain size was retained at 300 cm  $\times$  200 cm, but the infiltration was applied to the top left hand 60 cm of the surface boundary while the initial depth of water was fixed at 60 cm. Two levels of spatial discretization were used,  $\Delta x = 10$  cm and  $\Delta z = 10$  cm, and  $\Delta x = 20$  cm and  $\Delta z = 10$  cm. Both of these meshes were used to simulate the flow for 2 h using temporal discretization of  $\Delta t = 0.002$ , 0.02 and 0.1 h. The errors were compared to a fine mesh simulation; however, instead of using the pressure head directly as the fine solution; it was

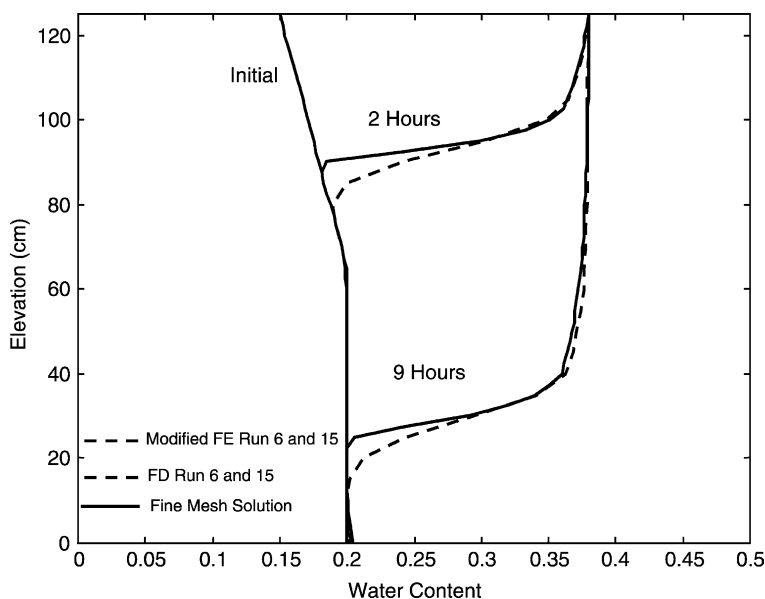


Fig. 6. Comparison of MFE and FD solutions to the field infiltration problem using a coarse numerical grid.

Table 2  
Results for the FD and MFE algorithm comparison for the modified Vauclin problem

Run	$\Delta x$ (cm)	$\Delta z$ (cm)	$\Delta t$ (h)	MFE error	FD error
19	10	10	0.002	0.000	0.363
20	10	10	0.020	0.259	1.744
21	10	10	0.100	468.2	519.3
22	20	10	0.002	1.706	4.965
23	20	10	0.020	2.023	9.243
24	20	10	0.100	139.3	860.7

the elevation of the phreatic surface that was used to calculate the error via Eq. (18). Table 2 summarizes the errors for all the numerical discretizations. For each profile, the error for the MFE solution is consistently smaller than the FD error. Fig. 7 shows the profiles obtained from the FD and MFE algorithms at a coarse discretization. The phreatic surface profiles show that the MFE solution is able to maintain a correct representation of the fine mesh solution, while the FD solution is prone to errors. Since this problem involves both flux boundaries and true two-dimensional flow, the improvement in the FE solution over the FD solution is attributed to a combination of the differences in hydraulic conductivity averaging and

the representation of the flux boundaries between the two algorithms.

In summary, this comparison shows that the MFE approach is superior to, and able to produce a more accurate solution than was possible using the FD approach for coarse discretizations. In certain cases the profiles obtained with a coarse MFE solution were able to maintain an accurate resemblance of the fine solution while the FD solution was quite erroneous. The explanation for the improved performance of the MFE solution is the incorporation of a larger spatial extent of the hydraulic conductivity variability and the difference in how FE methods represent specified flux boundaries. This kind of improved stability in FE solutions has been previously reported, (Cooley, 1983); however, it is of interest here to see the significance of the FD errors and the improvement offered by an FE solution. Re-writing the general FE equation as the MFE solution is useful to explicitly demonstrate how the FE solution automatically incorporates a more elaborate representation of the spatial variation of the hydraulic conductivity than the FD approach. This is important, particularly for infiltration problems that are characterized by steep wetting fronts and rapid spatial changes in the hydraulic conductivity.

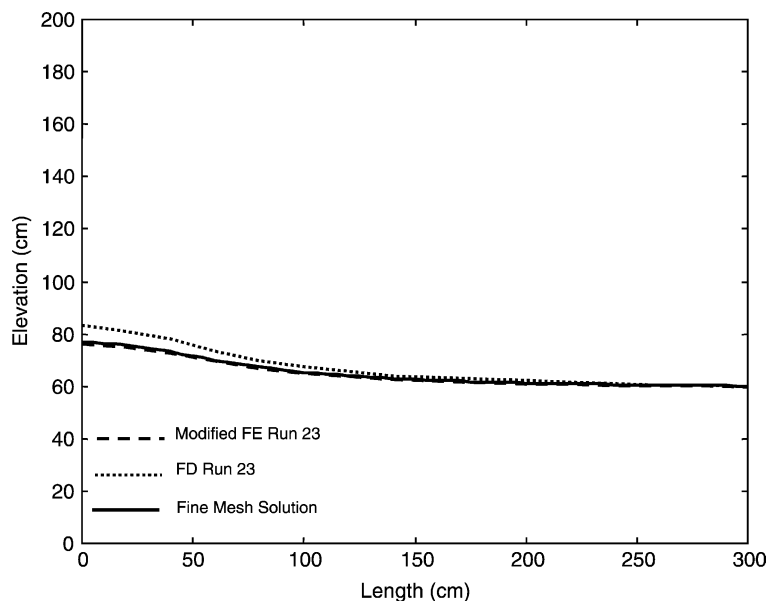


Fig. 7. MFE and FD solutions to the modified Vauclin infiltration problem under a coarse numerical grid.

## 5. Comparison of modified finite element and traditional finite element solutions

Since the use of the MFE algorithm is restricted in comparison to the standard FE solution, it should be noted that the standard FE procedure offers a more general and flexible solution to variably saturated flow problems. The general FE procedure can easily handle irregularly shaped domains, and irregular node spacing as well as allowing the material properties to change from element to element. None of these features are permitted with the MFE algorithm.

The MFE solution does offer several computational advantages as compared to the usual FE approach. The obvious difference is in the form of the resulting matrix equation. The stiffness matrix for the MFE solution is a penta-diagonal matrix that can be neatly stored as five vectors thereby avoiding the need to define and store the whole stiffness matrix. The penta-diagonal matrix can be efficiently solved using conjugate gradient algorithms that only require the facility to multiply the stiffness matrix and its transpose with an arbitrary vector (Press et al., 1992). This kind of storage and solution scheme is preferable to the standard FE methods where the stiffness matrix will be banded and sparse depending upon the node numbering scheme. Although conjugate gradient algorithms can be developed to efficiently store and solve banded and sparse equations, the MFE solution approach is much more straightforward and simple to implement.

One further limitation of the MFE algorithm is that it is restricted to meshes with uniform diagonal alignment; hence the element direction is biased. This could result in mesh-induced anisotropy issues when the mesh is coarse, a problem commonly encountered in traditional FE analysis (Boufadel et al., 1999). There are several ways to remedy this problem; firstly the use of symmetric elements, such as the bi-linear rectangular element, can eliminate the element bias. However, since we were interested in developing a 5-node relationship that was similar in nature to the FD approximation, this alternative was not pursued, as the bi-linear rectangular element would result in a 9-node relationship. Secondly the element alignment can be modified so that the direction of the diagonal is not uniform (Cooley, 1983). However, the uniform diagonal alignment was chosen as this ensured

the penta-diagonal structure of the resulting system of equations. Finally, it has been demonstrated that refining the element size in a uniformly aligned mesh can reduce the impact of the bias (Boufadel et al., 1999). This is the simplest method for minimizing the impact of alignment bias, and therefore it is recommended that a grid refinement study should always be undertaken to ensure that the chosen discretization is free from alignment-induced bias.

In summary, the MFE approach provides advantages over both the traditional FE and FD solutions for certain problems. The MFE algorithm is only applicable to those problems that can be discretized upon a regular domain, and therefore the use of the MFE algorithm faces the same limitations associated with the FD approach in this respect. However, in terms of performance, the MFE approach naturally provides a higher quality solution than the standard FD approach, and hence is a superior alternative for solving regular problems. In addition, the MFE algorithm provides advantages over the traditional FE approach for regular problems as the same quality solution associated with a uniformly aligned linear triangular mesh is obtained without the need for element/node numbering, pre-processing, or sparse matrix storage and solution schemes.

## 6. Conclusions

A comprehensive analysis of the solution of two-dimensional variably saturated flow problems by the FE and FD methods was undertaken. The analysis led to the development of an MFE algorithm for the solution of the two-dimensional variably saturated flow equation. The discrete MFE equations were derived to demonstrate the fundamental differences between the FD and FE discretization procedures. The MFE equations clearly show how the FE method naturally incorporates a broader spatial extent of the hydraulic conductivity variation as compared to the usual FD approximation. The algorithm was used to develop a code for solving two-dimensional variably saturated flow problems. The code was then benchmarked against the solutions of two standard variably saturated flow problems.

Once the MFE algorithm was validated, then the code was used in conjunction with a standard FD

approximation to evaluate the significance of the differences in the discrete equations. Two infiltration problems were solved several times using a range of spatial and temporal discretizations. The results from the MFE and FD algorithms were compared against known fine mesh solutions. The results showed that the algorithms performed equivalently for a one-dimensional problem, however the MFE solution was preferable for a two-dimensional problem solved upon a coarse grid. For the two-dimensional problem, the MFE algorithm was able to maintain a reasonable approximation to the fine mesh profile, while at the same discretization, the FD solution was plagued by numerical errors. Therefore this analysis showed that the errors introduced by an FD approximation can be significant and that the FE approach for the same numerical discretization can avoid these problems due to the intrinsic averaging of material properties and improved representation of specified flux boundaries.

In addition to the comparison of the FD and MFE algorithms, some specific advantages of the MFE algorithm have also been illustrated. Firstly, any traditional FE algorithm used with the same discretization as the MFE is inefficient compared to the MFE algorithm. This is because the MFE approach generates a simple matrix equation that can be stored and solved using elementary numerical schemes without resorting to dealing with sparse matrices. Secondly, solutions from the standard FD algorithm are numerically inferior to those obtained using the MFE approach because of how the two approaches approximate the partial differential equation. Therefore, any problem that can be discretized upon a regular grid is most efficiently solved using the proposed MFE algorithm.

### Acknowledgements

We would like to thank the Journal of Hydrology reviewers Dr R.L. Cooley and Prof. F.J. Molz for their useful comments. We would also like to thank Dr L.R. Townley and Dr D.A. Reynolds for their initial review of the material. This work was made possible by the support provided by the Australian Postgraduate Award through the Centre for Water Research and the University of Western Australia.

### References

- Boufadel, M.C., Suidan, M.T., Venosa, A.D., 1999. Numerical modeling of water flow below dry salt lakes: effect of capillarity and viscosity. *Journal of Hydrology* 221, 55–74.
- Celia, M.A., Bouloutas, E.T., Zarba, R.L., 1990. A general mass-conservative numerical solution of the unsaturated flow equation. *Water Resources Research* 26, 1483–1496.
- Clement, T.P., Wise, W.R., Molz, F.J., 1994. A physically based, two-dimensional, finite-difference algorithm for modeling variably saturated flow. *Journal of Hydrology* 161, 71–90.
- Cooley, R.L., 1983. Some new procedures for numerical solution of variably saturated flow problems. *Water Resources Research* 19 (5), 1271–1285.
- Cooley, R.L., 1992. A modular finite-element model (MODFE) for areal and axisymmetric ground-water flow problems, Part 2: derivation of finite-element equations and comparisons with analytical solutions. US Geological Survey, Techniques of Water-Resources Investigations, Book 6, Chapter A4.
- Eisenberg, M.A., Malvern, L.E., 1973. On finite element integration in natural coordinates. *International Journal for Numerical Methods in Engineering* 7, 574–575.
- Gray, W.G., 1984. Comparison of Finite Difference and Finite Element Methods. In: Bear, J., Coropcioglu, M.Y. (Eds.), *Fundamentals of Transport Phenomena in Porous Media*, NATO Advanced Science Institutes Series, Martinus Nijhoff Publishers, The Netherlands, pp. 899–952.
- Haverkamp, R., Vauclin, M., 1981. A comparative study of three forms of the Richard equation used for predicting one-dimensional infiltration in unsaturated soil. *Soil Science Society of America Journal* 45, 13–20.
- Hayhoe, H.N., 1978. Study of the relative efficiency of finite difference and Galerkin techniques for modeling soil-water transfer. *Water Resources Research* 14 (1), 97–102.
- Istok, J., 1989. *Groundwater Modelling by the Finite Element Method*, American Geophysical Union, Washington.
- Mualem, Y., 1976. A new model for predicting hydraulic conductivity of unsaturated porous media. *Water Resources Research* 12, 513–522.
- Neuman, S.P., 1973. Saturated–unsaturated seepage by finite elements. *Journal of the Hydraulics Division, Proceedings of the American Society of Civil Engineers* 99, 2233–2250.
- Neuman, S.P., Feddes, R.A., Bresler, E., 1975. Finite element analysis of two-dimensional flow in soils considering water uptake by roots: 1 theory. *Soil Science Society of America Proceedings* 39, 224–230.
- Pinder, G.F., Gray, W.G., 1976. Is there a difference in the finite element method? *Water Resources Research* 12 (1), 105–107.
- Press, W.H., Flannery, B.P., Teukolsky, S.A., Vetterling, W.T., 1992. *Numerical Recipes in Fortran, The Art of Scientific Computing*, second ed, Cambridge University Press, Cambridge.
- Segerlind, L.J., 1984. *Applied Finite Element Analysis*, second ed, Wiley, New York.
- Segol, G., 1976. A three-dimensional Galerkin-finite element model for the analysis of contaminant transport in saturated–unsaturated porous media. *Finite Elements in Water Resources*, 2.123–2.144.

- Simpson, M.J., 2002. An analysis of unconfined groundwater flow characteristics about a seepage-face boundary. Draft PhD Thesis, Centre for Water Research, University of Western Australia, Perth, Australia.
- Van Genuchten, M.Th., 1980. A closed form equation for predicting the hydraulic conductivity of unsaturated soils. *Soil Science Society of America Journal* 44, 892–898.
- Van Genuchten, M.Th., 1982. A comparison of numerical solutions of the one-dimensional unsaturated–saturated flow and mass transport equations. *Advances in Water Resources* 5 (1), 46–55.
- Vauclin, M., Khanji, D., Vauchaud, G., 1979. Experimental and numerical study of a transient two-dimensional unsaturated–saturated water table recharge problem. *Water Resources Research* 15 (5), 1089–1101.
- Wang, H.F., Anderson, M.P., 1982. *Introduction to Groundwater Modeling: Finite Difference and Finite Element Methods*, Freeman, San Francisco.
- Warrick, A.W., Biggar, J.W., Nielsen, D.R., 1971. Simultaneous solute and water transfer for an unsaturated soil. *Water Resources Research* 7 (5), 1216–1225.
- Zheng, C., Bennett, G.D., 1995. *Applied Contaminant Transport Modeling: Theory and Practice*, Van Nostrand Reinhold, New York.
- Zienkiewicz, O.C., Cheung, Y.K., 1965. Finite elements in the solution of field problems. *The Engineer*, 507–510.